UNIVERSITY
OF TRENTO

DEPARTMENT OF INFORMATION AND COMMUNICATION TECHNOLOGY

38050 Povo – Trento (Italy), Via Sommarive 14
http://www.dit.unitn.it

A MULTI-SOURCE STRATEGY BASED ON A LEARNING-BY-EXAMPLES TECHNIQUE FOR BURIED OBJECT DETECTION

Emanuela Bermani, Andrea Boni, Salvatore Caorsi, Massimo Donelli, and Andrea Massa

August 2004

Technical Report DIT-04-067

A Multi-Source Strategy based on a Learning-by-Examples Technique for Buried Object Detection

Emanuela Bermani*, Andrea Boni*, Salvatore Caorsi**, Massimo Donelli*, and Andrea Massa*

* Department of Information and Communication Technology

University of Trento

Via Sommarive, 14

38050 Trento - ITALY

E-mail: *andrea.massa@ing.unitn.it*

** Department of Electronics

University of Pavia

Via Ferrata, 1

27100 Pavia - ITALY

A Multi-Source Strategy based on a Learning-by-Examples Technique for Buried Object Detection

Emanuela Bermani, Andrea Boni, Salvatore Caorsi, Massimo Donelli, and Andrea Massa

Abstract

In the framework of buried object detection and subsurface sensing, some of the main difficulties in the reconstruction process are certainly due to the aspect-limited nature of available measurement data and to the requirement of an on-line reconstruction. To limit these problems, a multi-source (MS) learning-by-example (LBE) technique is proposed in this paper. In order to fully exploit the more attractive features of the MS strategy, the proposed approach is based on a support vector machine (SVM). The effectiveness of the MS-LBE technique is evaluated by comparing the achieved results with those obtained by means of a previously developed single-source (SS) SVM-based procedure for an ideal as well as a noisy environment.

1 Introduction

The detection of natural as well as man-made subsurface targets, the identification of cracks and voids included in a host structure, the location of sedimentary layers under the sea water represent few examples of a large number of practical applications where the reconstruction of an unknown object embedded in a not-accessible region is required.

As a matter of fact, the arising problem can be reformulated in terms of an inverse scattering problem where the problem-unknowns (i.e., the image of the subsurface target) are obtained starting from the observation of the electromagnetic interactions between the object and a probing electromagnetic source. However, a large set of subsurface retrieval problems, unlike standard imaging problems, presents some peculiar requirements and characteristics:

- the aspect-limited measurement setup (and, consequently, a limited achievable information content);
- the need of a real-time processing.

As far as the information achievable from scattered data is concerned, due to the system geometry (being both electromagnetic sources and measurement points located on the same half-space), the inverse-problem data are acquired only on a finite set of measurement positions (aspect-limited data) resulting in a troublesome reconstruction process [1] particularly if a single-source single-illumination strategy is taken into account.

In order to enhance the reconstruction accuracy, enlarging the information content of the input data, a MS strategy can be usefully adopted. As a matter of fact, single-source multi-illumination strategies have been already successfully employed in the framework of conventional inverse scattering problems [2][3]. However, when conventional nonlinear single-source multi-illumination inverse scattering techniques are used, large computational resources are required strongly limiting the possibility for a real or quasi-real-time processing. Then, to fully exploit the effectiveness of a microwave imaging method, allow-ing an on-line detection also for large values of the contrast function, the use of so-called LBE techniques results very attractive. The detection problem is reformulated into a regression one, where the data (i.e., the measures of the anomalous field) and the unknowns (i.e., the position of the object as well as its geometric and dielectric characteristic according to the adopted parameterization) are related by means of an approximated function to be estimated through an off-line data fitting process (*training phase*). As a matter of fact, approaches based on both neural networks (NNs) [5][6] and SVMs [7][8] have been satisfactorily applied for buried object detection in presence of single-illumination acquisition systems. On the other hand, the use of a multi-illumination strategy certainly would improve the localization accuracy of the LBE-based approach, but could greatly complicate the mandatory training procedure. Consequently, in order to increase the data information content jointly limiting the overall computational burden during the training phase, an innovative, to the best of authors' knowledge, LBE-approach based on a multi-source strategy is taken into account in this paper.

In more detail, the manuscript is organized as follows. Starting from the description of the detection problem (Sect. 2), Section 3 presents the mathematical formulation of the multi-source SVM-based approach. After a deep assessment of the potentialities and current limitations of the method (Sect. 4), some conclusions and final remarks are reported in Section 5.

2 Formulation of the Regression Problem

Let us consider the half-space geometry shown in Figure 1, where the upper region is assumed to be free-space ($\varepsilon_{r1} = 1.0$, $\sigma_1 = 0.0$) and the lower region is representative of a lossy ground, whose relative permittivity and electric conductivity are ε_{r2} and σ_2, respectively. A two-dimensional circular cylinder of diameter d_{cil} is buried in the lossy earth at an unknown position $\underline{\rho}_{cil} = x_{cil}\underline{\widehat{x}} + y_{cil}\underline{\widehat{y}}$. The transmitters and receivers are located in the free-space, along a straight line parallel to the air-earth interface. Moreover, let us suppose that the buried cylinder is contained in an investigation domain $D_I = \left\{-\frac{L}{2} \leq x \leq \frac{L}{2}; -\frac{L}{2} \leq y \leq \frac{L}{2}\right\}$. Consequently, the permittivity distribution of the investigation domain results

$$\varepsilon_{D_I}\left(\underline{\rho}\right) = \begin{cases} \varepsilon_{rcil} & \underline{\rho} \in S_{cil} \\ \varepsilon_{r2} & otherwise \end{cases} \tag{1}$$

$$\sigma_{D_I}\left(\underline{\rho}\right) = \begin{cases} \sigma_{cil} & \underline{\rho} \in S_{cil} \\ \sigma_{2} & otherwise \end{cases} \tag{2}$$

where S_{cil} indicates the cylinder cross-section.

Then, by assuming $\hat{\underline{z}}$-directed electric current filaments as electromagnetic sources, the scattered electric field measured at the rth receiver position $\underline{\rho}_r$, $r = 1, ..., R$ due to T transmitters located at $\underline{\rho}_t$, $t = 1, ..., T$ is given by

$$E_{scat}\left(\underline{\rho}_r\right) = k^2 \int_{D_I} G_{12}\left(\underline{\rho}_r, \underline{\rho}\right) \, E\left(\underline{\rho}_t \, t = 1, ..., T; \underline{\rho}\right) \, O\left(\underline{\rho}\right) \, d\underline{\rho} \tag{3}$$

where $E\left(\underline{\rho}_t \, t = 1, ..., T; \underline{\rho}\right)$ is the electric field at $\underline{\rho} \in D_I$ due to the illumination produced by T sources; $G_{12}\left(\underline{\rho}_r, \underline{\rho}\right)$ is the Green function when $\underline{\rho}_r$ belongs to the upper half-space and $\underline{\rho}$ lies in the ground; $O\left(\underline{\rho}\right)$ is the object function defined as follows

$$O\left(\underline{\rho}\right) = O_{\varepsilon}\left(\underline{\rho}\right) + j\frac{1}{\omega\varepsilon_{r1}} O_{\sigma}\left(\underline{\rho}\right) \tag{4}$$

where $O_{\varepsilon}\left(\underline{\rho}\right) = \varepsilon_{D_I}\left(\underline{\rho}\right) - \varepsilon_{r2}$ and $O_{\sigma}\left(\underline{\rho}\right) = \sigma_{D_I}\left(\underline{\rho}\right) - \sigma_2$.

The detection problem is aimed at determining the unknown function relating the measurement data to the unknowns of the inverse scattering problem, that is to find a function $\Im$ such that:

$$\underline{\wp} = \Im\left(\underline{\Gamma}_E\right) \tag{5}$$

being $\underline{\wp} = \left\{\underline{\rho}_{cil}, \, d_{cil}, \, \varepsilon_{rcil}, \, \sigma_{cil}\right\}$ and $\underline{\Gamma}_E = \left\{E_{scat}\left(\underline{\rho}_r\right), r = 1, ..., R\right\}$. The arising problem is very complex and difficult to be managed due to the nonlinearity and ill-posedness. However, if N examples (i.e., couples of input-output pairs $\left\{\left(\underline{\wp}\right)_n, \left(\underline{\Gamma}_E\right)_n\right\}$, $n = 1, ..., N$) are available, then (5) can be seen as an example of a regression problem for which an approximation of $\Im$ can be determined by means of a SVM-based procedure as detailed in Sect. 3.

3 LBE-based Technique for Buried Object Detection - The SVM Algorithm

Learning-by-examples techniques are based on the following underlying idea: "*to find an approximation of the unknown function* $\Im$ *by means of a data-fitting process*".

As far as the NN approach [9] is concerned, the data fitting is carried out by means of a nonlinear interpolation of the N examples in the $R-$dimensional input space, $\underline{\Gamma}_E$, (being R the input-space dimension). However, NN-based solution generally does not allow the model complexity control, sometime leading to an "over-fitting" of the training data and resulting in an inability to correctly estimate the output in presence of input data which do not belong to the original training set.

Conversely, SVMs maintain generalization properties by considering a linear data-fitting in a transformed space where the original examples are mapped through a nonlinear mapping. In more detail, firstly each data array $\{\underline{\Gamma}_E\}_n$ is mapped into the so-called "feature space" by means of a nonlinear transformation $\underline{\varphi} : \Re^R \rightarrow \Re^{\widetilde{R}}$ being $\widetilde{R} \gg R$. Then, the sample points on the feature space are linearly interpolated according to the following relation

$$\widehat{\Im}\left(\underline{\Gamma}_E\right) = \underline{w} \cdot \underline{\varphi}\left(\underline{\Gamma}_E\right) + b \tag{6}$$

where $\underline{w}$ is the vector normal to the hyper-plane defined by (6) in the feature space and b is the bias term. The selection of the proper hyper-plane is carried out by solving the arising constrained minimization problem:

$$min_{\underline{w}} \left\{ \Omega\left(\underline{w}\right) \right\} \tag{7}$$

under the constraints

$$\left\{ \begin{array}{c} \left| \wp_n^{(k)} - \left(\underline{w} \cdot \underline{\varphi} \left\{ \left(\underline{\Gamma}_E \right)_n \right\} + b \right) \right| \leq \epsilon + \xi_n \\ \xi_n \geq 0 \end{array} \right. \tag{8}$$

where

$$\Omega\left\{\underline{w}\right\} = \Omega_1\left\{\underline{w}\right\} + \lambda\,\Omega_2\left\{\underline{w}\right\} = \frac{1}{2}\left\|\underline{w}\right\|^2 + \lambda \sum_{n=1}^{N} \xi_n \tag{9}$$

being $\wp_n^{(k)}$ the kth component of the nth target of the training set. Then, it results that the so defined hyper-plane is "as flat as possible" (thus providing a simple linear data fitting in the feature space) and the arising approximating function $\widehat{\Im}$ shows for a large number of examples a deviation from the target lower than a fixed quantity, ϵ, and greater deviations, ξ_n, for some examples.

In order to solve (7), the original problem is usually reformulated in its "dual form" by introducing N Lagrange multipliers, α_n, $n = 1, \ldots N$ (see [10] for a detailed mathematical description)

$$\begin{array}{c} max_{\alpha_n} \left\{ \Psi\left(\alpha_n,\ n = 1, \ldots N\right) \right\} = max_{\alpha_n} \left\{ \frac{1}{2} \sum_{i=1}^{N} \sum_{j=1}^{N} \alpha_i\, \alpha_j K \left(\underline{\varphi} \left\{ \left(\underline{\Gamma}_E \right)_i \right\}, \underline{\varphi} \left\{ \left(\underline{\Gamma}_E \right)_j \right\} \right) + \right. \\ \left. + \epsilon \sum_{n=1}^{N} \left| \alpha_n \right| - \sum_{n=1}^{N} \alpha_n \wp_n^{(k)} \right\} \end{array} \tag{10}$$

$$\sum_{n=1}^{N} \alpha_n = 0 \qquad \alpha_n \in \left[-\lambda, \lambda\right] \tag{11}$$

where $K\left(\underline{x}_i, \underline{x}_j\right) = \underline{\varphi}\left(\underline{x}_i\right) \cdot \underline{\varphi}\left(\underline{x}_j\right)$ is the *kernel* function. Provided that K be positive-defined, the quadratic problem (10)-(11) has an unique solution and standard algorithms [11][12] can be used in order to determine the α_n coefficients. Consequently, it is possible to analytically express $\underline{w}$ as follows

$$\underline{w} = \sum_{n=1}^{N} \alpha_n \underline{\varphi}\left\{(\underline{\Gamma}_E)_n\right\} \tag{12}$$

and to compute the value of the bias term, b, according to [12]

$$b = \wp_n^{(k)} - \sum_{j=1}^{N} \left[\alpha_j \underline{\varphi}\left\{(\underline{\Gamma}_E)_n\right\} \cdot \underline{\varphi}\left\{(\underline{\Gamma}_E)_j\right\} - \epsilon \cdot sign\left(\alpha_n\right)\right]. \tag{13}$$

According to (6) and (12), the approximating function $\widehat{\Im}$ can be rewritten as

$$\widehat{\Im}\left(\underline{\Gamma}_E\right) = \sum_{n=1}^{N} \alpha_n K\left\{(\underline{\Gamma}_E)_n, \underline{\Gamma}_E\right\} + b \tag{14}$$

where only the knowledge of *support vectors*, $\{\alpha_j \neq 0,\ j = 1, ..., J\}$, and of the kernel function is needed. It should be pointed that its is not required to explicitly define the nonlinear function $\underline{\varphi}$ and the nonlinear mapping is realized by selecting a function K so that it represents a positive-definite kernel function. In this paper, gaussian kernel functions, whose effectiveness in dealing with subsurface sensing has been already assessed [5], are taken into account.

4 Results

In order to test the effectiveness of the proposed approach, a set of selected numerical examples is considered . With reference to the problem geometry illustrated in Figure 1, the following geometry and dielectric parameters are taken into account. The subsurface relative permittivity and conductivity are $\varepsilon_{r2} = 4.0$ and $\sigma_2 = 1\, mS/m$, respectively. The investigation domain is a $\lambda \times \lambda$ square region where an unknown lossless circular pipe, $d_{cil} = \lambda/6$ in diameter and characterized by a relative permittivity equal to $\varepsilon_{rcil} = 5.0$, is located. The multi-source system is organized as follows. Transmitters and receivers are located at $h_t = h_r = \lambda/6$ above the air-earth interface and $R = 16$ receivers are positioned along the linear observation domain ($L = \lambda$ long) with an inter-element distance equal to $\Delta_r = \lambda/15$. Moreover, illuminating sources are positioned one $\lambda/4$ far from the other ($\Delta_t = \lambda/4$) on the same linear domain. The measurement data are numerically computed by means of a finite-element-based simulator and by considering an additive white gaussian noise with assigned signal-to-noise ratio (SNR) to simulate a realistic noisy environment.

As far as the generation of the training and of the test sets are concerned, the target cylinder is moved in $N_{train} = 676$ and $N_{test} = 625$ different positions according to the following scanning rule

$$\underline{\rho}_n^{(i)} = \left(x_{pq}^{(i)}, y_{pq}^{(i)}\right) \qquad n = 1, ..., N^{(i)} \tag{15}$$

where the super-script i is related to the "training" ($train$) or to the "test" ($test$), and

$$\begin{cases} x_{pq}^{(i)} = x_{start}^{(i)} + (p-1)\,\Delta x^{(i)} \qquad p = 1, ..., N_x^{(i)} \\ y_{pq}^{(i)} = y_{start}^{(i)} + (q-1)\,\Delta y^{(i)} \qquad q = 1, ..., N_y^{(i)} \\ N^{(i)} = N_x^{(i)} \times N_y^{(i)} \end{cases} \tag{16}$$

being $x_{start}^{(train)} = y_{start}^{(train)} = -\lambda/2$, $\Delta x^{(train)} = \Delta y^{(train)} = \lambda/25$, $N_x^{(train)} = N_y^{(train)} = 26$, and $x_{start}^{(test)} = y_{start}^{(test)} = -12\lambda/25$, $\Delta x^{(test)} = \Delta y^{(test)} = \lambda/25$, $N_x^{(test)} = N_y^{(test)} = 25$, respectively.

In the first test case, $T = 3$ unit sources, located so that the medium one is central with respect to the investigation domain, are considered in an almost ideal environment scenario ($SNR = 100\,dB$) to preliminary assess the effectiveness of the proposed multi-source LBE-based approach (MSLBE). To this end, in order to allow a quantitative estimation of the localization accuracy, the following error figures are then defined

- *Local Errors*

$$\delta_x^n = \frac{|x_{pq} - \widetilde{x}_{pq}|}{D} \qquad \delta_y^n = \frac{|y_{pq} - \widetilde{y}_{pq}|}{D} \qquad \begin{array}{c} n = p + (q-1)N_x^{(test)} \\ p = 1, ..., N_x^{(test)} \\ q = 1, ..., N_y^{(test)} \end{array} \tag{17}$$

being $(\widetilde{x}_{pq}, \widetilde{y}_{pq})$ and (x_{pq}, y_{pq}) estimated and actual coordinates of the scatterer, respectively, and $D = L$ the maximum error.

- *Local Average Errors*

$$\Delta_x^p = \frac{\left| X_p - \frac{1}{N_y^{(test)}} \sum_{r=1}^{N_y^{(test)}} \widetilde{x}_{pr} \right|}{D} \qquad p = 1, ..., N_x^{(test)} \tag{18}$$

$$\Delta_y^p = \frac{\left| Y_q - \frac{1}{N_x^{(test)}} \sum_{r=1}^{N_x^{(test)}} \widetilde{y}_{rq} \right|}{D} \qquad q = 1, ..., N_y^{(test)} \tag{19}$$

where $X_p = x_{pq}$, $\forall q = 1, ..., N_y^{(test)}$ and $Y_q = y_{pq}$, $\forall p = 1, ..., N_x^{(test)}$.

- *Global Average Errors*

$$\Theta_x = \frac{1}{D} \sqrt{\frac{1}{N_y^{(test)}} \sum_{p=1}^{N_y^{(test)}} \left[X_p - \frac{1}{N_y^{(test)}} \sum_{r=1}^{N_y^{(test)}} \widetilde{x}_{pr} \right]^2} \tag{20}$$

$$\Theta_y = \frac{1}{D} \sqrt{\frac{1}{N_x^{(test)}} \sum_{q=1}^{N_x^{(test)}} \left[Y_q - \frac{1}{N_x^{(test)}} \sum_{r=1}^{N_x^{(test)}} \widetilde{y}_{rq} \right]^2} \tag{21}$$

Figure 2 shows the local error in the estimation of both the target coordinates as a function of the target position. For comparison purposes, the results obtained with a single-source single-illumination LBE-based approach (SSLBE) are also reported in Figure 3 (being the unit source located at a central position with respect to the investigation domain). As can be observed, the MSLBE technique generally outperforms the SSLBE approach. In particular, the horizontal resolution results very accurate as confirmed from the local error statistics (Tab. I) $\frac{1}{3}$ lower than those related to SSLBE approach.

As far as the robustness to the environmental noise is concerned, the performances of the proposed approach are evaluated in the second test case dealing with a training data set related to examples with $SNR = 100\,dB$ but test sets ranging from $SNR = 100\,dB$ to $SNR = 5\,dB$. Figure 4 shows the behavior of the global average error in the estimation of the spatial x and y coordinates as a function of the signal-to-noise ratio. As a comparison, the plots related to SSLBE approach are also reported. It can be noted that the MSLBE approach guarantees an improvement in the localization accuracy also in correspondence with lower SNR values. In more detail, if the use of the multiple source strategy allows a consistent decrease in the localization error along the horizontal direction, it retains the good performances already shown by SSLBE in the estimation of the target depth, slightly improving the localization effectiveness for strongly noisy environments.

Since the prediction of the horizontal position of the target is more positively affected by the MSLBE strategy, in order to better understand the arising positive "effects", the relative local average is reported in Figure 5. As expected, in correspondence with a fixed signal-to-noise, the MSLBE approach better estimates the position of the targets located near the lateral boundaries of the investigation domain with a corresponding local average error lower than 0.05 for $SNR \geq 10\,dB$ when $-0.3 \leq \frac{X_p}{\lambda} \leq 0.25$.

5 Conclusions

In this paper a multi-source LBE-based electromagnetic approach is presented for the detection of buried objects. The proposed method allows to combine the advantages of a multi-source strategy with those of a SVM-based methodology, satisfying the requirements of both accurate and real-time processing. The effectiveness of the approach has been assessed, also in comparison with a previously developed SSLBE approach, by considering noiseless as well as noisy environments. The obtained results demonstrated an improved accuracy regardless to the modeled environmental noise and, particularly, in predicting the horizontal coordinate of the target. Future research activities will be devoted to the definition of the optimal trade-off between number and location of illumination sources in order to give some guidelines for the design of optimized sub-surface electromagnetic applicators.

References

[1] N. V. Budko and P. M. van den Berg, "Estimation of the average contrast of a buried object," *Radio Science*, vol. 35, no. 2, pp. 547-555, 2000.

[2] T. J. Cui, W. C. Chew, A. A. Aleaddin, and S. Chen, "Inverse scattering of two-dimensional dielectric objects buried in a lossy earth using the distorted Born iterative method," *IEEE Trans. on Geoscience and Remote Sensing*, vol. 39, no. 2, pp. 339-346, 2001.

[3] S. Caorsi, G. L. Gragnani, and M. Pastorino, "An electromagnetic imaging approach using a multi-illumination technique," *IEEE Trans. Biomedical Engineering*, vol. 41, pp. 406-409, 1994.

[4] C. -C. Chiu and C. -P. Huang, "Inverse scattering of dielectric cylinders buried in a half-space," *Microwave and Optical Tech. Lett.*, vol. 13, no. 2, pp. 96-99, 1996.

[5] E. Bermani, S. Caorsi, and M. Raffetto, "An inverse scattering approach based on a neural network technique for the detection of dielectric cylinders buried in a lossy half-space," in *Progress in Electromagnetic Research*, vol. 26, pp. 69-90, 2000.

[6] I. T. Rekanos, "Inverse scattering of dielectric cylinders by using radial basis function neural networks," *Radio Science*, vol. 36, no. 5, pp. 841-849, 2001.

[7] E. Bermani, A. Boni, S. Caorsi, and A. Massa, "An innovative real-time technique for buried object detection" *IEEE Trans. on Geoscience and Remote Sensing*, vol. 41, no. 4, pp. 927-931, 2003.

[8] S. Caorsi, D. Anguita, E. Bermani, A. Boni, M. Donelli, and A. Massa, "A comparative study of NN and SVM-based electromagnetic inverse scattering approaches to on-line detection of buried objects," *Journal of the Applied Computational Electromagnetics Society*, Special Issue on "*Neural Network Applications in Electromagnetics*," vol. 18, no. 2, pp. 1-11, 2003.

[9] C. Christodoulou and M. Georgiopoulos. *Applications of Neural Networks in Electromagnetics.* Boston, Artech House, 2001.

[10] V. N. Vapnik. *The Nature of Statistical Learning Theory.* John Wiley & Sons, New York, 1999.

[11] J. Platt, "Fast training of support vector machines using sequential minimal optimization," in *Advances in Kernel Methods - Support Vector Learning*, The MIT Press (Eds. B. Schölkopf, C. Burges, A. Smola), 1999.

[12] D. Mattera, F. Palmieri, and S. Haykin, "An explicit algorithm for training support vector machines," *IEEE Signal Processing Letters*, vol. 6, no. 9, pp. 243-245, 1999.

Figure Captions

- Figure 1 - Problem geometry.
- Figure 2 - MSLBE approach. Local error as a function of the actual position of the buried cylinder: (a) δ_x and (b) δ_y.
- Figure 3 - SSLBE approach. Local error as a function of the actual position of the buried cylinder: (a) δ_x and (b) δ_y.
- Figure 4 - Behavior of the global average error versus SNR: (a) Θ_x and (b) Θ_y.
- Figure 5 - Behavior of the horizontal local average error in correspondence with various SNR values: (a) MSLBE approach and (b) SSLBE approach.

Table Captions

- Table I - Local error statistics.

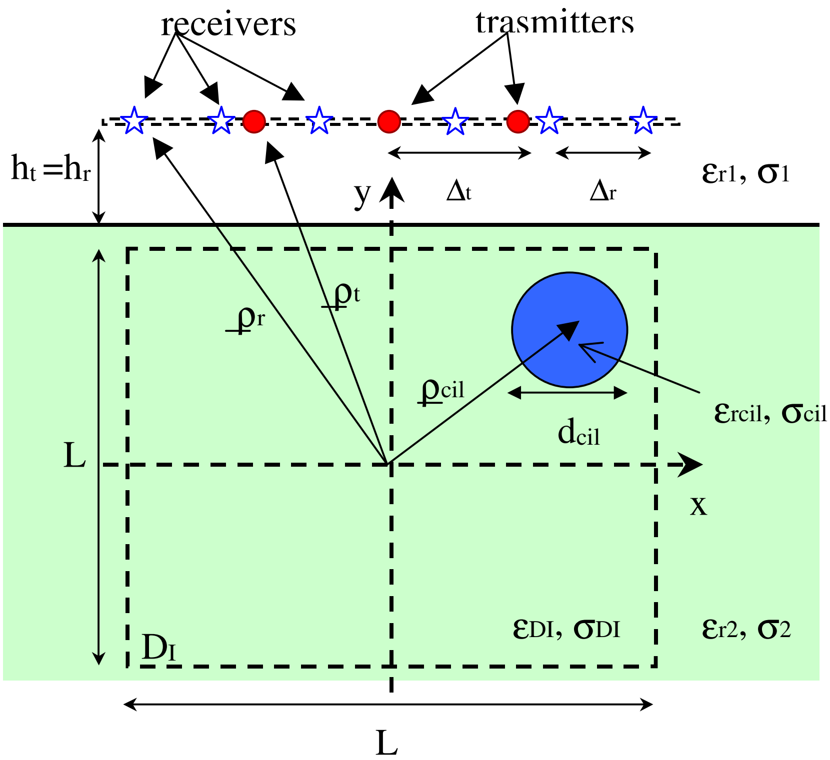

Fig. 1 - E. Bermani *et al.*, "A Multi-Source Approach based on ..."

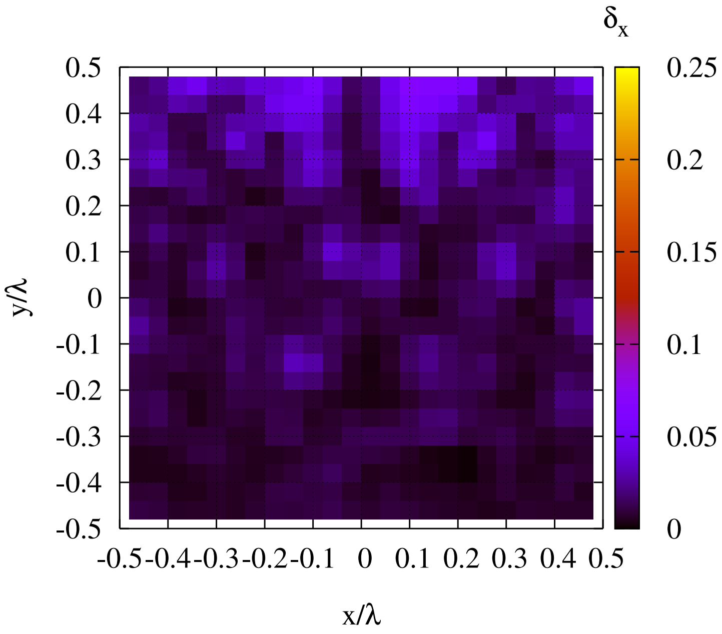

(a)

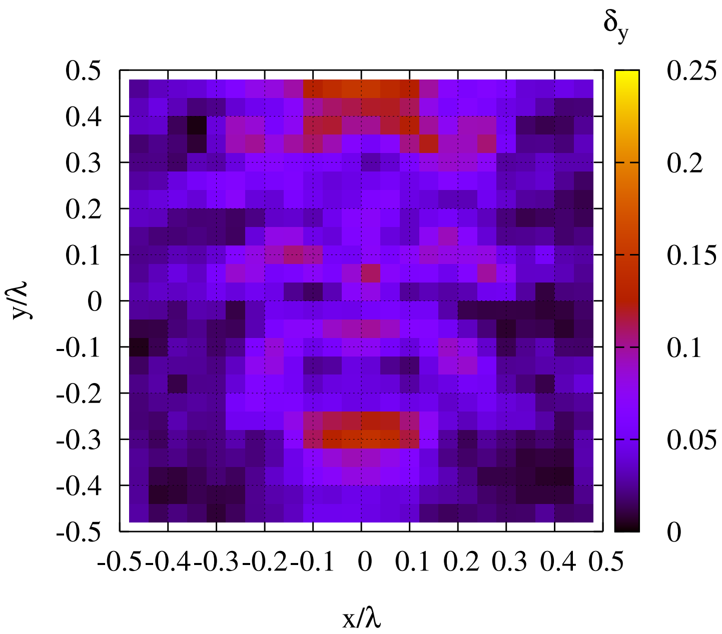

(b)

Fig. 2 - E. Bermani *et al.*, "A Multi-Source Approach based on ..."

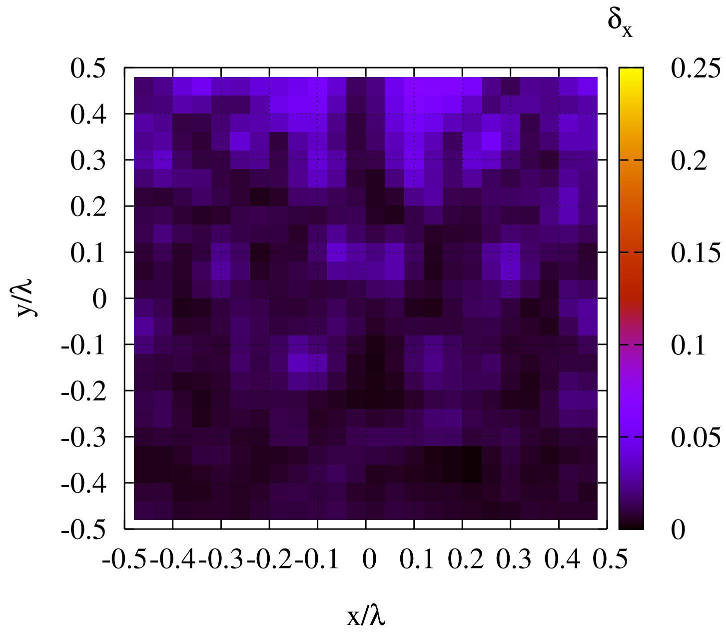

(*a*)

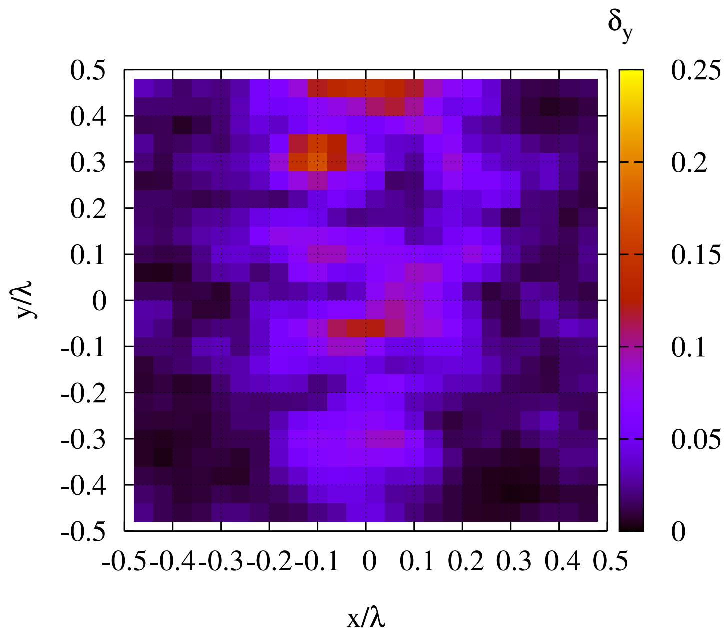

(*b*)

Fig. 3 - E. Bermani *et al.*, "A Multi-Source Approach based on ..."

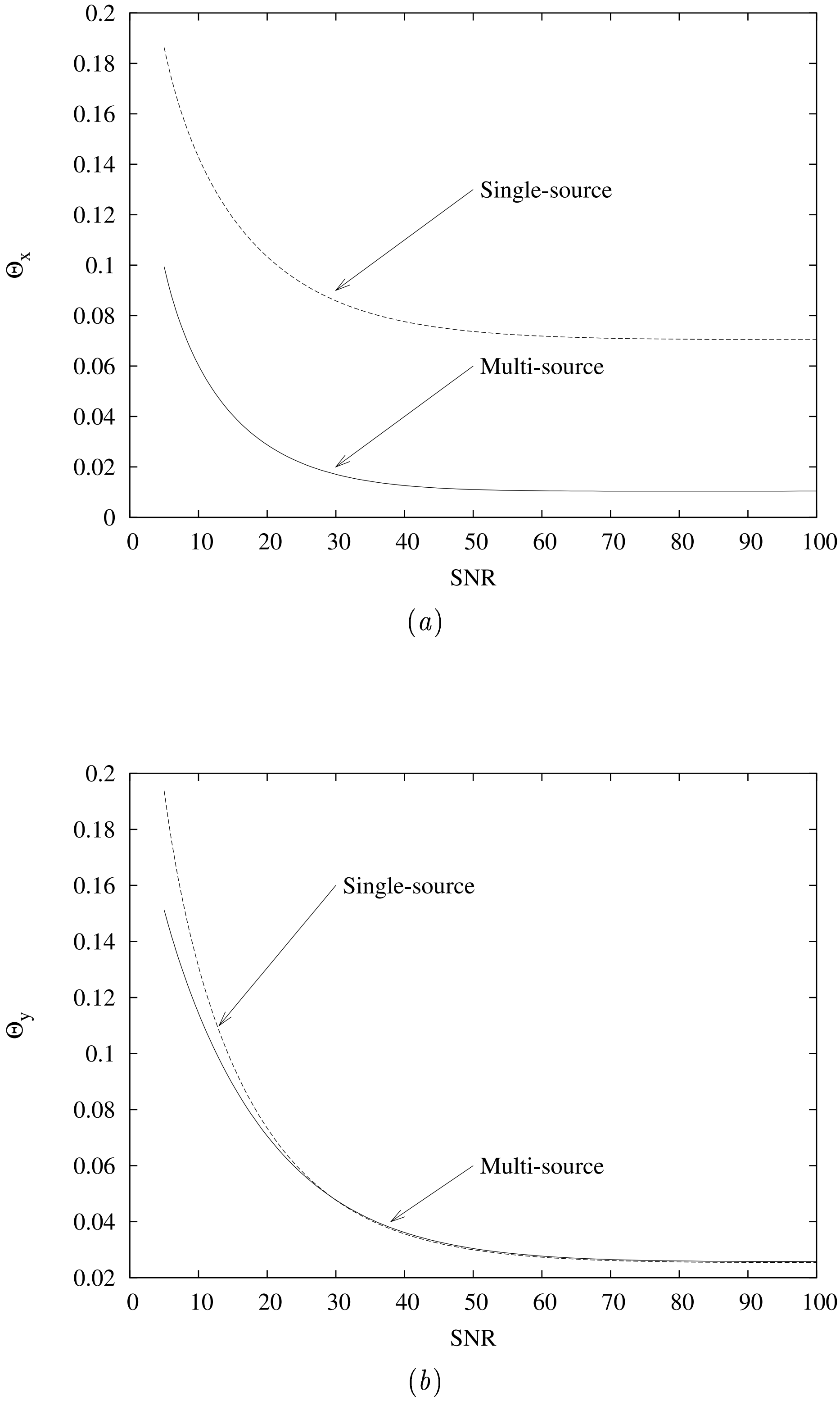

Fig. 4 - E. Bermani *et al.*, "A Multi-Source Approach based on ..."

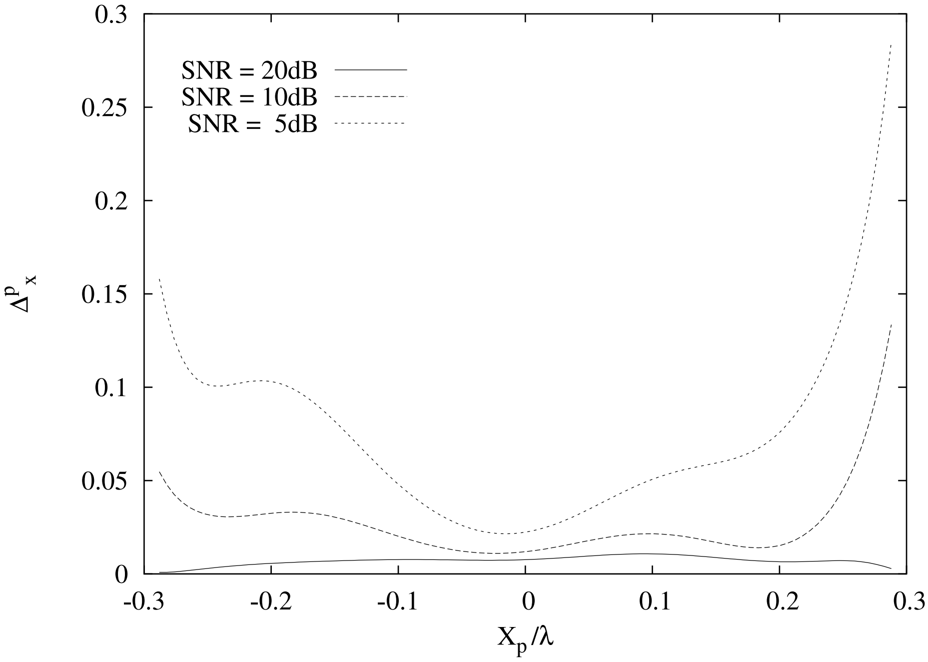

(a)

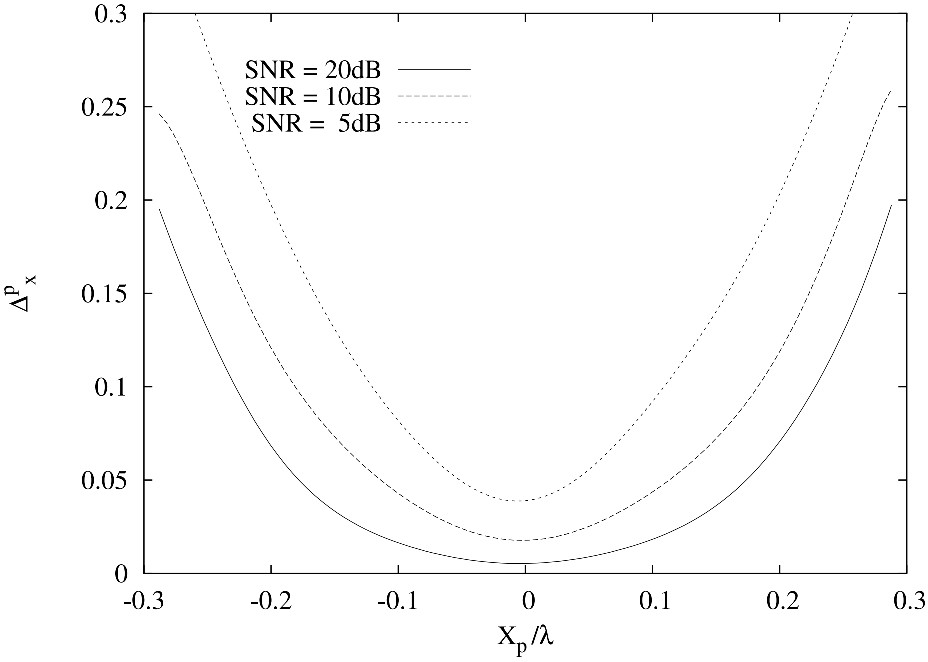

(b)

Fig. 5 - E. Bermani *et al.*, "A Multi-Source Approach based on ..."

	$av_n\left\{\delta_x^n\right\}$	$max_n\left\{\delta_x^n\right\}$	$min_n\left\{\delta_x^n\right\}$
$MSLBE - Approach$	0.015	0.079	7.55×10^{-5}
$SSLBE - Approach$	0.058	0.274	6.80×10^{-5}

(a)

	$av_n\left\{\delta_y^n\right\}$	$max_n\left\{\delta_y^n\right\}$	$min_n\left\{\delta_y^n\right\}$
$MSLBE - Approach$	0.035	0.207	1.56×10^{-5}
$SSLBE - Approach$	0.035	0.224	3.09×10^{-5}

(b)

Tab. I - E. Bermani *et al.*, "A Multi-Source Approach based on ..."